ACS APPLIED MATERIALS & INTERFACES

Research Article

www.acsami.org

Aqueous Combustion Synthesis of Aluminum Oxide Thin Films and Application as Gate Dielectric in GZTO Solution-Based TFTs

Rita Branquinho,* Daniela Salgueiro, Lídia Santos, Pedro Barquinha, Luís Pereira, Rodrigo Martins, and Elvira Fortunato*

CENIMAT/I3N Departamento de Ciência dos Materiais, Faculdade de Ciências e Tecnologia (FCT), Universidade Nova de Lisboa (UNL), and CEMOP/UNINOVA, 2829-516 Caparica, Portugal

Supporting Information

ABSTRACT: Solution processing has been recently considered as an option when trying to reduce the costs associated with deposition under vacuum. In this context, most of the research efforts have been centered in the development of the semiconductors processes nevertheless the development of the most suitable dielectrics for oxide based transistors is as relevant as the semiconductor layer itself. In this work we explore the solution combustion synthesis and report on a completely new and green route for the preparation of amorphous aluminum oxide thin films; introducing water as solvent. Optimized dielectric layers were obtained for a water based precursor solution with 0.1 M concentration and demonstrated high capacitance, 625 nF cm^{-2} at 10 kHz, and a permittivity of 7.1. These thin films were successfully applied as gate dielectric in solution processed gallium−zinc-tin oxide (GZTO) thin film transistors (TFTs) yielding good electrical performance such as subthreshold slope of about 0.3 V dec^{-1} and mobility above 1.3 cm^2 V^{-1} s^{-1}.

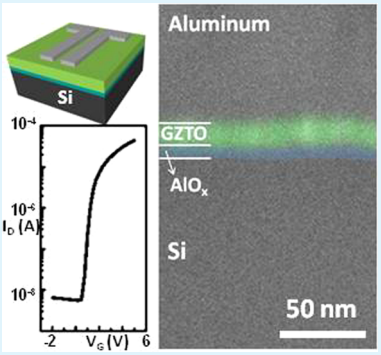

KEYWORDS: *combustion reaction, aqueous synthesis, aluminum oxide, solution TFTs, GZTO*

1. INTRODUCTION

The evolution from rigid silicon-based electronics to low-cost flexible electronics requires the use of solution-based production methods. Recently, there has been remarkable development in solution-processed inorganic metal oxide semiconductor materials for high-performance thin film transistors (TFTs) and such devices have demonstrated impressive results,[1−8] including indium free ones,[9,10] which in some cases are comparable to or even surpass the ones obtained by physical techniques.[11] However, the development of dielectrics by solution processing is still a step behind, inhibiting the deposition of all the layers using the same technology.

High-κ metal oxide-based insulators have demonstrated high performance and suitability for application in metal oxide semiconductor based TFTs.[11−13] Solution-processed oxide precursor routes have been reported for several high κ dielectrics; sodium beta-alumina,[14] Al_2O_3,[15,16] HfO_2,[17] Ta_2O_5, Nb_2O_5, $NbTaO_5$,[18] ZrO_2;[19] however, high temperatures (above 400 °C) are still required for degradation of the organic load. Lowering the organic content can be achieved by using aqueous precursor solutions free of undesirable couterions and organic groups, as reported for HfO_2, TiO_2 and $Al_4O_3(PO_4)_2$,[20,21] ZnO,[8] and most recently for In_2O_3.[22]

Solution combustion synthesis has been widely used for the development of oxide powder materials for diverse applications, such as catalysis and solid oxide fuel cells.[23−25] This combustion synthesis takes advantage of the chemistry of the solution precursors as a source of energy for localized heating. The exothermic reaction of a metal nitrate, which provides the metal ions and also acts as oxidizer, with a fuel (acetylacetone or urea) generates energy that can convert precursors into oxides at lower process temperatures. Theoretically this reaction mechanism can be applied to any metal ion to produce the desired oxide.[23−25]

The application of this synthesis to the production of thin films has been reported for semiconductor materials such as indium oxide and indium, zinc tin and gallium-based multicomponent oxides,[1,4] indium yttrium oxide[2,3] thin films, and most recently for a dielectric material, AlO_x.[26] The precursor solutions are obtained by dissolution of the desired metal salts and fuel (acetylacetone or urea) in an organic solvent, 2-methoxyethanol (2-ME) and annealing at mild temperatures yields the metal oxide. High performance TFTs were obtained with solution processed metal oxide semiconductor thin films annealed at temperatures as low as 200 °C.[1] The use of aqueous precursor solutions for oxide synthesis has been

In this work, we report the solution combustion synthesis of amorphous AlO_x thin films (dielectric) using for the first time environmental friendly water-based precursors, as typically used for bulk solution combustion synthesis of oxides.[23−25] For comparison, 2-methoxyethanol was also used as solvent, as reported for semiconductor oxides.[1,4] The properties and quality of produced thin films are highly dependent on the

Received: June 17, 2014
Accepted: October 29, 2014
Published: October 29, 2014

precursor solution characteristics, hence the influence of the solutions concentration (from 0.05 to 0.5 M) and aging time (from as prepared to 30 days aging) were studied for both solvents, water and 2-methoxyethanol (2-ME). The application of optimized solution based amorphous AlO_x thin films as gate dielectric in solution processed semiconductor oxide TFTs is also demonstrated.

2. EXPERIMENTAL DETAILS

2.1. Precursor Solution Preparation and Characterization. Aluminum nitrate nonahydrate ($Al(NO_3)_3{\cdot}9H_2O$, Fluka, 98%) was dissolved in 25 mL of solvent, either 2-methoxyethanol (2-ME, $C_3H_8O_2$, Fluka, 99%) or deionized water, to yield solutions with an Al^{3+} ion concentration of 0.05, 0.1, 0.25 and 0.5 M. Urea ($CO(NH_2)_2$, Sigma, 98%) was then added to the prepared solutions which were maintained under constant stirring for at least 1 h. The urea to aluminum nitrate molar proportion was 2.5:1 for each concentration to guarantee the redox stoichiometry of the reaction. The as prepared precursor solutions were then allowed to age for 3, 15, and 30 days. Prior to their use, all solutions where magnetically stirred for 15 min and filtrated through 0.45 μm hydrophilic filters. Thermal and chemical characterization of precursor solutions were performed by thermogravimetry and differential scanning calorimetry (TG-DSC) and Fourier Transform Infra-Red (FT-IR) spectroscopy. TG-DSC analysis were performed under air atmosphere up to 500 °C with a 5 °C/min heating rate in an aluminum crucible with a punctured lid using a simultaneous thermal analyzer, Netzsch (TG-DSC - STA 449 F3 Jupiter). FT-IR data were recorded using an Attenuated Total Reflectance (ATR) sampling accessory (Smart iTR) equipped with a single bounce diamond crystal on a Thermo Nicolet 6700 Spectrometer. The spectra were acquired with a 45° incident angle in the range of 4000−650 cm^{-1} and with a 4 cm^{-1} resolution.

2.2. Thin Film Deposition and Characterization. Prior to deposition all substrates (silicon wafer and soda-lime glass) were cleaned in an ultrasonic bath at 60 °C in acetone for 15 min, then in 2-isopropanol for 15 min and dried under N_2; followed by a 30 min. UV/Ozone surface activation step using a PSD-UV Novascan system. Thin films were deposited by spin coating a single layer of the AlO_x precursor solutions for 35 s at 2000 rpm (Laurell Technologies) followed by an immediate hot plate annealing at 350 °C for 30 min in ambient conditions.

The films' structure was assessed by glancing angle X-ray diffraction (GAXRD) performed by an X'Pert PRO PANalytical powder diffractometer using with Cu Kα line radiation (λ = 1.540598 Å) with angle of incidence of the X-ray beam fixed at 0.9°. The surface morphology was investigated by atomic force microscopy (AFM, Asylum MFP3D) and scanning electron microscopy (SEM, Zeiss Auriga Crossbeam electron microscope).

Spectroscopic ellipsometry measurements of thin films deposited on silicon substrates were made over an energy range of 1.5−6.0 eV with an incident angle of 70° using a Jobin Yvon Uvisel system. The acquired data were modulated using the DELTAPSI software using a two layer model (with standard reference for silicon) and a classical single oscillator dispersion formula to simulate the dielectric response of AlO_x. The fitting procedure was done pursuing the minimization of the error function (χ^2).[27] ATR FT-IR spectroscopy characterization of thin films deposited on glass substrates was performed as described for precursor solutions.

2.3. Electronic Device Fabrication and Characterization. Metal−insulator-semiconductor (MIS) capacitors were produced by AlO_x thin film deposition onto p-type silicon substrates (1−10 Ω cm) as described above (see section 2.2). Aluminum gate electrodes (100 nm thick) with an area of 8.7×10^{-3} cm^2 were deposited by thermal evaporation via shadow mask. A 100 nm thick aluminum film was also deposited on the back of the silicon wafer to improve electrical contact. Electrical characterization was performed measuring both the capacitance−voltage and capacitance-frequency characteristics in the range off 10 kHz to 1 MHz of the devices using a semiconductor characterization system (Keithley 4200SCS).

The TFTs were produced in a staggered bottom-gate, top-contact structure by depositing AlO_x thin films onto p-type silicon substrates (1−10 Ω cm) as described above. The gallium zinc tin oxide (GZTO) semiconductor layer was deposited by sequentially spin coating (for 35 s at 2000 rpm) four layers of GZTO (0.1:2.0:1.0) precursor solution 0.05 M onto the AlO_x thin films and annealed in air at 350 °C for 30 min after each layer deposition. Finally, source and drain aluminum electrodes (100 nm thick) were deposited by e-beam evaporation via shadow mask onto annealed films, defining a channel width (W) and length (L) of 1400 and 100 μm, respectively. The current−voltage characteristics of the devices were obtained in continuous mode with both back and forth sweeps recorded in ambient conditions inside a Faraday cage using a semiconductor parameter analyzer (Agilent 4155C). The saturation mobility (μ_{SAT}) was determined from the following equation[28]

$$I_D = \left(\frac{C_i W \mu_{SAT}}{2L}\right)(V_G - V_T)^2 \quad (1)$$

where C_i is the gate dielectric capacitance per unit area, W and L are the channel width and length, V_G is the gate voltage and V_T is the threshold voltage, which was determined in the saturation region by linear fitting of a $I_D^{1/2}$ vs V_G plot.

3. RESULTS AND DISCUSSION

Solution combustion synthesis is a method to obtain metal oxides that takes advantage of the chemistry of the solution precursors as a source of energy for localized heating. The exothermic chemical reaction between a solution of the desired metal salts, usually nitrates, which provide the metal ions and also act as oxidizer and an organic fuel (reducing agent), generates energy that can convert precursors into oxides at lower process temperatures.[1,23,24]

The solution combustion synthesis of Al_2O_3 from aluminum nitrate and urea can be represented by the combination of aluminum nitrate decomposition reaction (eq 2) and urea oxidation reaction (eq 3)

$$2Al(NO_3)_3{\cdot}9H_2O \rightarrow Al_2O_3 + 18H_2O + 3N_2 + \left(\frac{15}{2}\right)O_2 \quad (2)$$

$$CO(NH_2)_2 + \left(\frac{3}{2}\right)O_2 \rightarrow 2H_2O + CO_2 + N_2 \quad (3)$$

The overall reaction can thus be written as bellow (eq 4)

$$2Al(NO_3)_3{\cdot}9H_2O + CO(NH_2)_2 \rightarrow Al_2O_3 + 20H_2O + CO_2 + 4N_2 + 6O_2 \quad (4)$$

It should be pointed out that this is a theoretical reaction equation that neglects possible secondary reactions such as urea hydrolysis, thermal decomposition, fuel-oxidizer adduct and also nitrates decomposition however it allows the calculation of a stoichiometric condition that can be used as a reference.[23]

The chemistry of the redox reaction is determinant for the thermodynamics of the oxide formation; namely the nature of the reagents and the fuel/oxidizer ratio (Φ). The relation between the redox stoichiometry and the molar ratio of reagents can be determined by the reducing/oxidizing valencies (RV/OV) of the reagents and is given by

$$\Phi = \frac{RV}{OV}n \quad (5)$$

where n is the number of moles of fuel per mole of oxidizer.[23−25]

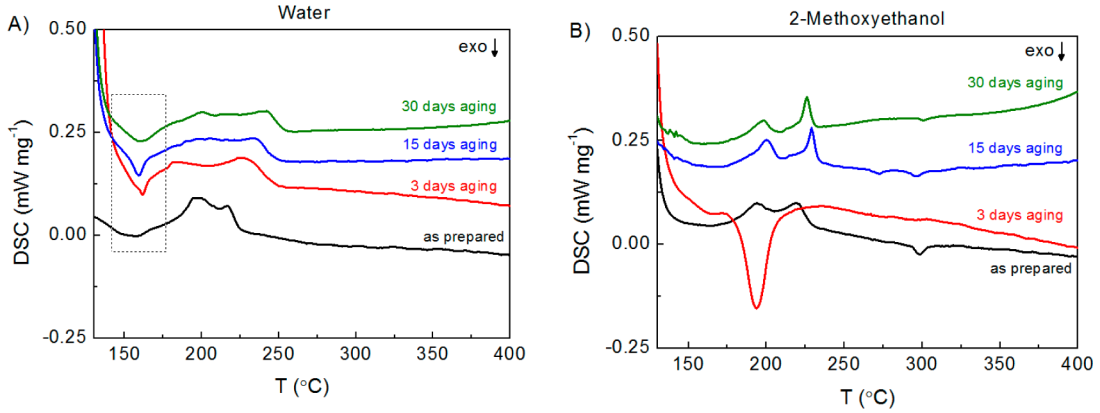

Figure 1. DSC analysis of (A) water and (B) 2-methoxyethanol-based AlO_x precursor solutions with 0.1 M concentration and different aging time: as-prepared, 3, 15, and 30 days.

The optimal stoichiometry composition of the redox mixture is obtained for $\Phi = 1$, meaning that no molecular oxygen is required. The oxidizing/reducing characteristics of a mixture can be calculated by the Jain method,[29] which is based on propellant chemistry.[23−25] In this method carbon and hydrogen are considered as reducing elements with final valences of +4 and +1, respectively; metal ions are also considered reducing elements with their respective valence. Oxygen and nitrogen are considered oxidizers with their final valences of −2 and 0, respectively.[23−25] The reducing valence of urea is +6 and the oxidizing valence of aluminum nitrate is −15 as calculated by the Jain method hence 2.5 mol of urea are required per mole of aluminum nitrate to ensure redox stoichiometry. This 2.5 urea to aluminum nitrate molar ratio was maintained constant while investigating the influence of the precursor solution solvent; water and 2-methoxyethanol (2-ME); the metal ion concentration; 0.05−0.5 M, and the solution aging time (as prepared to 30 days aging) on the synthesis and properties of alumina thin films.

3.1. Precursor Solution Characterization. Precursor solutions were characterized by ATR FT-IR spectroscopy in order to assess chemical changes in the solution composition with aging time and reagents concentration, before film's production. FT-IR spectra of single reagents in water and 2-ME solution where obtained to allow precursor solution spectra interpretation. Generally, precursor solutions spectra represent the sum of the initial reagents solution spectra with only slight deviations. As expected, specific urea and nitrate vibration bands intensity increase with precursor solution concentration however no apparent modification related to changes of the aluminum ion coordination sphere could be noted in the FT-IR spectra associated with precursor solution aging time. This was observed for both water (see Figure S1 in the Supporting Information) and 2-ME-based precursor solutions (see Figure S2 in the Supporting Information).

Thermal analysis of precursor solutions was performed by TG-DSC. Although there should be major differences between the precursor decomposition processes in bulk and thin film form, as reported by Sanchez-Rodriguez et al.,[30] thermal analysis of precursor solutions in the same conditions used in thin film deposition (without a prior concentration/drying step) was performed to assess the influence of the aging time. Generally the TG-DSC results are dominated by endothermic events related to the high solvent to reagents ratio. Solvent evaporation was identified for all solutions as an endothermic event, with correspondent weight loss above 90%, which occurs at 100−110 °C and 126−131 °C for water and 2-ME based precursors, respectively. Closer analysis of differential scanning calorimetry (DSC) results allows the identification of exothermic events for AlO_x precursor solutions with a 0.1 M concentration and different aging time as depicted in Figure 1. Here data bellow 130 °C is not presented to avoid the event associated with endothermic solvent evaporation.

Water-based AlO_x precursor solutions (Figure 1A) show similar thermal characteristics regardless of solution aging time, namely, an exothermic event at 155−165 °C, which represents the combustion reaction (indicated by the dotted rectangle) and endothermic events at 217−245 °C attributed to the decomposition of residual fuel. The combustion process involves several phenomena which are not accounted for in the simplified eq 4 such as urea hydrolysis, thermal decomposition, fuel-oxidizer adduct, and nitrates decomposition.[23] These secondary reactions could lead to the variation of initial fuel-to-oxidizer ratio resulting in residual fuel.

For 2-ME based AlO_x precursors (Figure 1B) the lowest reaction temperature; 194 °C, is obtained for a 3 days aging time meaning that solution aging time is a relevant parameter in the combustion reaction of 2-ME based precursors. Kim et al. proposed that when the metal salts are dissolved in 2-ME a ligand exchange reaction from nitrate to 2-methoxyethoxide or hydroxide occurs;[31] this change in the metal ion coordination sphere explains the need for an aging time. Three days aging time appears to be the optimal time for the ligand exchange reaction to occur since for other aging times an exothermic event occurs at higher temperatures (295−300 °C) and endothermic events at 195−230 °C are also observed. Although the detailed reaction mechanism is not completely understood, reports on 2-ME-based metal oxide precursors usually allow an aging process prior to film deposition without a scientific explanation.[1,4,31] Water-based AlO_x precursors show combustion reaction temperature 25 °C lower than that of 2-ME-based AlO_x precursor which can be related to the specific bonding energy of the 2-methoxyethoxide ligands to the aluminum ions as reported by Epifani et al. for copper precursors prepared with different ligands.[25]

3.2. Thin Film Characterization. Thin film thickness was determined by spectroscopic ellipsometry using a two layer model (with standard reference for silicon) and a classical single oscillator dispersion formula to simulate the dielectric response of AlO_x (Figure 2).

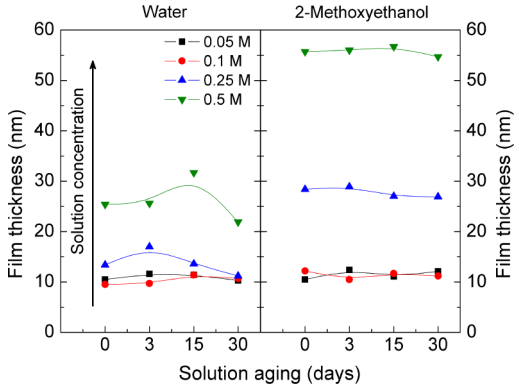

Figure 2. AlO_x thin films thickness variation with precursor solution concentration and aging time for both solvents, water and 2-methoxyethanol.

For low precursor solution concentrations, 0.05−0.1 M, about 10 nm thick films are obtained for both water and 2-ME-based AlO_x. Increasing the precursor concentration leads to thicker films with this effect being more pronounced for 2-ME-based solutions which is related to its higher viscosity (η = 1.375 mPa s at 30 °C) when compared to water (η = 0.7975 mPa s at 30 °C).[32] Precursor solution aging does not significantly affect film thickness for either solvent. Due to the nature of the reaction a higher uniformity might be expected for thinner films, which can be advantageous for device applications.

GAXRD analysis of thin films showed that amorphous films are obtained regardless of precursor solution solvent, aging or concentration (Figure 3).

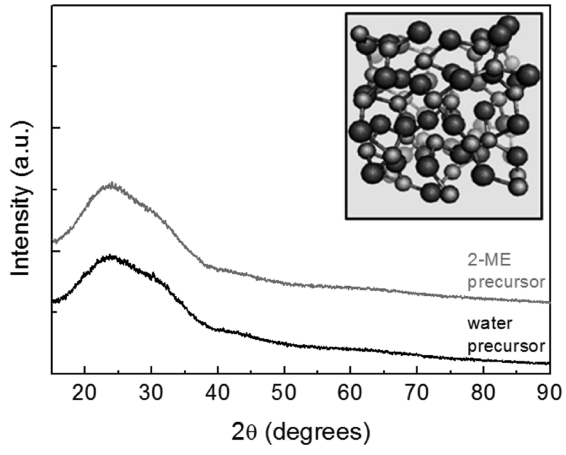

Figure 3. GAXRD analysis of water and 2-methoxyethanol (c = 0.1 M) solution-based AlO_x thin films deposited on soda-lime glass substrates. The inset shows a schematic of a typical amorphous AlO_x molecular structure. Large spheres represent oxygen atoms, and small ones aluminum atoms (adapted from ref 33).

FT-IR spectra of produced films are presented in Figure 4. It can be seen that for high solution concentration ($c \geq 0.25$ M) initial reagents traces remain within the films meaning that the reaction is not complete (Figure 4B). This effect is less pronounced for films produced from water-based solutions (Figure 4A). The presence of nitrate ions in the AlO_x thin films was identified through the asymmetric stretching of nitrate, expected at 1340−1390 cm^{-1},[25,34] which was attributed to a sharp vibration band at 1357 cm^{-1}. This is inconsistent with thermal analysis results obtained for bulk precursor solutions that show no changes above 250 °C, which also emphasizes the difference between bulk and film decomposition processes. The presence of nitrates within solution processed alumina thin films annealed at 350 °C has been reported by Park et al.[16] who demonstrated that the presence of $-NO_3^-$ facilitates water adsorption which was also identified herein through the −OH broad vibration bands at 3450 and 1630 cm^{-1}.[16,34]

The morphology of AlO_x thin films depends on the precursor solution solvent as demonstrated by SEM analysis of water and 2-ME-based films produced from as prepared precursor solutions with a Al^{3+} concentration of 0.1 M (Figure 5).

AlO_x thin films produced from water-based precursors are smooth and uniform (Figure 5A) with an even distribution of aluminum throughout the film (Figure 5B). The surface morphology is maintained with increasing solution's aging time and concentration. A four layered water-based AlO_x sample was produced to assess layer thickness by SEM. The total film thickness obtained was 44 nm in average which amounts to about 11 nm per layer for water-based AlO_x (Figure 5C) being in good agreement with spectroscopic ellipsometry data for single layered thin films. 2-ME precursor solutions yield less uniform films as depicted in Figure 5D. The observed features might arise from a less uniform reaction because of higher organic load of 2-ME. AFM measurements (see Figure S3 in the Supporting Information) showed that a slightly higher surface roughness is obtained for 2-ME based films (0.9 nm) when compared to water based films (0.3 nm). Also water based films demonstrated higher refractive index (see Figure S4 in the Supporting Information), which can be related to an increased density when compared to 2-ME based films.

3.3. MIS Characterization. The influence of precursor solutions concentration and aging time on the dielectric properties of solution based AlO_x was assessed by electrical characterization of MIS capacitors with Si/AlO_x/Al structure obtained by depositing one layer of solution based AlO_x onto p-type silicon substrates and annealing on a hot plate at 350 °C for 30 min. Generally, thin films obtained from precursor solutions with high concentration ($c \geq 0.25$ M) demonstrate poor dielectric properties which can be related to the presence of the initial reagents within the films, as demonstrated by FT-IR analysis (Figure 4).

Capacitance-frequency measurements (see Figure S5 in the Supporting Information) revealed that insulator capacitance increases for lower frequency, indicating the contribution of ionic polarization. Overall, we notice a large capacitance frequency dependence on both process routes followed at low frequencies for an aging time of 3 days, which can be associated with a possible ionic charge defects increase. Nevertheless, for intermediate frequency range we notice the presence of a plateau where the capacitance and relative permittivity obtained for 10 nm thick films of water and 2-ME based AlO_x at 10 kHz are 7.1 and 4.7, respectively (see Table S1 in the Supporting Information). The permittivity values are lower than expected for Al_2O_3, ∼9;[35] however, these are in agreement with reported values for solution processed Al_2O_3.[36] The nature of the combustion reaction and the release of gaseous products are expected to lead to some nanoporosity within the films which results in a lower permittivity.

The capacitance−voltage characteristics of the MIS structure were taken at a frequency of 1 MHz, following the usual procedure done in silicon based devices.[28] Under these

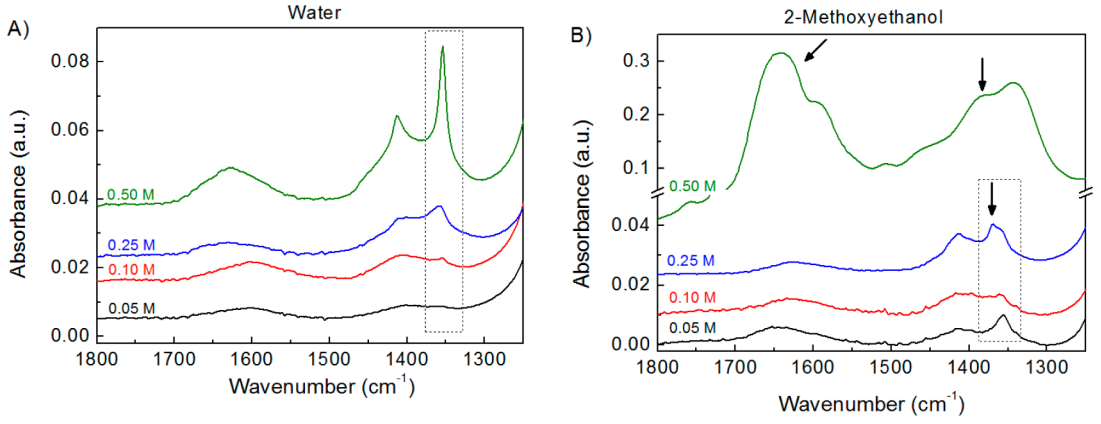

Figure 4. FTIR analysis of (A) 2-methoxyethanol and (B) water solution-based AlO_x thin films produced with as prepared precursor solutions (no aging) of various concentrations. Arrows indicate initial reagent vibration bands and dotted square denotes the asymmetric stretching of nitrate.

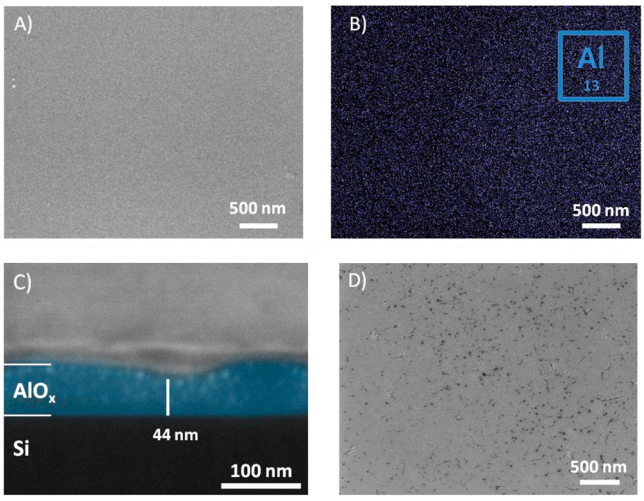

Figure 5. SEM analysis of AlO_x thin film produced from as prepared 0.1 M precursor solutions. (A) Surface morphology of one layered water-based AlO_x thin film; (B) aluminum distribution in A obtained by EDS mapping; (C) high-resolution FIB cross-section image of a four layer water-based AlO_x thin film; (D) surface morphology of one layered 2-methoxyethanol-based AlO_x thin film.

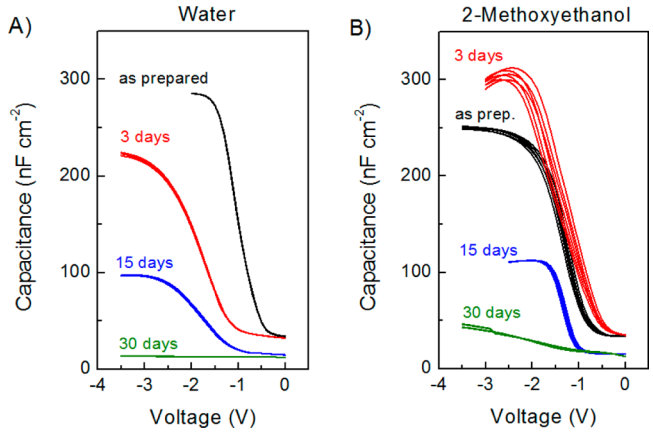

Figure 6. Capacitance–voltage characteristics of p-Si/AlO_x/Al MIS capacitors produced from (A) water-based and (B) 2-methoxyethanol-based precursor solutions with 0.1 M concentration and different aging time (for each sample 3 sequential loop measurements registered with a frequency of 1 MHz are shown; in the case of water, these are fully coincident).

conditions, the $C-V$ measurements taken using dielectrics produced from precursor solutions with 0.1 M concentration and different aging time were measured and for each sample three sequential loop curves are presented in Figure 6. Increasing solution aging time leads to lower capacitance and threshold voltage shift toward lower potentials indicating an increase in oxide charge defects and variations in the films' oxidation state.[13,28] Water-based films (Figure 6A) demonstrated high capacitance, stability and negligible hysteresis when compared to 2-ME based films (Figure 6B). In fact, when using water as solvent there is no need for precursor solution aging to attain higher capacitance. The leakage current density of p-Si/AlO_x/Al MIS capacitors produced from as prepared water-based precursor solutions with 0.1 M concentration (see Figure S6 in the Supporting Information) was determined to be 7.6×10^{-5} A/cm^2 when a 1 MV/cm electric field was applied. The observed leakage current arises from the reduced film thickness and the presence of nitrate groups within the film that facilitate water adsorption, as demonstrated by FTIR analysis (Figure 4). Nevertheless, the mechanism is not yet fully understood and further analysis is required.

3.4. TFT Characterization. AlO_x thin films produced from as prepared water-based precursor solutions with 0.1 M concentration demonstrated optimal characteristics as such their application in TFTs was studied. Bottom gate TFTs with solution-based GZTO semiconductor and optimized water-based AlO_x were produced on highly doped p-Si (gate electrode); TFTs with thermally grown SiO_2 were also produced for comparison. Aluminum source/drain contacts (100 nm) were used in all devices. Figure 7 shows high-resolution FIB-SEM cross-section images and transfer characteristics of these devices. Electrical characterization was performed in continuous mode with both back and forth sweeps recorded in ambient conditions in the dark.

SEM cross-section images of produced TFTs (Figure 7A,B) show the devices' layers. The GZTO semiconductor layer thickness was 17–18 nm in both devices and the measured SiO_2 thickness was 105 nm. The AlO_x dielectric layer could not be distinguished from silicon because of the atomic number proximity and reduced thickness of the film; however, it has been artificially highlighted in the SEM image to represent the device structure.

Successful gate modulation is obtained for all TFTs as demonstrated by devices' transfer characteristics (Figure 7C,

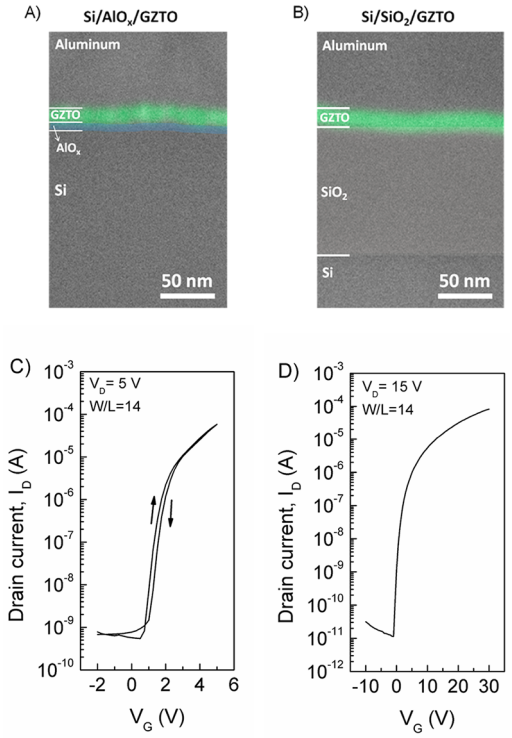

Figure 7. (A, B) High-resolution FIB-SEM cross-section images and (C, D) transfer characteristics of bottom gate TFTs produced on highly doped p-Si (gate) with solution-based GZTO and (A, C) water-based AlO_x; (B, D) thermally grown SiO_2. 100 nm thick aluminum source/drain contacts were used in all devices. FIB-SEM images are artificially highlighted for a better understanding.

D). Moreover, we notice a low hysteresis on the set of devices fabricated (ΔV = 0.2 V) in line to what was verified on the C−V characteristics. TFT performance is assessed trough the analysis of the turn-on voltage (V_{ON}), the threshold voltage (V_T), drain current on−off ratio (I_{ON}/I_{OFF}), subthreshold slope (S) and saturation mobility (μ_{SAT}), which was calculated using AlO_x capacitance at the 10 kHz in order to minimize overestimation. Bottom gate solution processed GZTO TFTs were produced with thermally grown SiO_2 to serve as a benchmark, as this is the most commonly used gate dielectric for TFTs assessment. These devices demonstrated V_{ON} = −1 V, V_T = 0.6 V, I_{ON}/I_{OFF} = 7.4 × 10^6, S = 0.5 V dec^{-1}, and μ_{SAT} = 0.7 cm^2 V^{-1} s^{-1}. The combination of solution processed AlO_x dielectric and GZTO semiconductor yielded TFTs with low hysteresis (0.2 V) and a good overall performance; V_{ON} = 0.5 V, V_T = 0.8 V, I_{ON}/I_{OFF} = 8.7 × 10^4, S = 0.3 V dec^{-1}, and μ_{SAT} = 1.3 cm^2 V^{-1} s^{-1}. The high I_{OFF} observed mainly arises from the use of nonpatterned semiconductor and gate electrode layers. This can be improved by implementing patterning techniques for all the device layers. Nevertheless, these devices demonstrated very good characteristics such as close to zero turn-on voltage, low subthreshold slope and saturation mobility above 1 cm^2 V^{-1} s^{-1}, which are achieved with low operation voltages due to the higher capacitance obtained with very thin AlO_x films. The results clearly show aqueous solution-processed AlO_x as a promising gate dielectric for application in solution processed devices.

Gate bias stress tests (Figure 8) were performed in ambient conditions on these devices by applying a constant gate voltage equivalent to a 2 MV cm^{-1} electric field for 3 h, after which the devices were allowed to recover. Transfer characteristics were measured at selected times during stress and recovery processes, in the dark (Figure 8A).

The V_T shift during stress is consistent with a charge trapping mechanism at the dielectric/semiconductor interface. Output characteristics obtained after recovery (Figure 8B) exhibit saturation behavior for all the V_G range, as required for reliable operation of a broad range of circuits. The small current crowding observed for low V_D is due to non-negligible gate leakage current at these voltage levels. This also has the natural effect of raising the off-current level of the transfer characteristics (Figure 7) and should be improved in the future with thicker AlO_x layer or/and a multilayer approach.[37]

4. CONCLUSIONS

In this work, we have demonstrated for the first time the aqueous combustion solution synthesis of aluminum oxide thin films at mild annealing temperature of 350 °C and their application in solution-processed GZTO TFTs. AlO_x thin films prepared from aqueous precursors showed enhanced properties, high stability, and an oxide formation reaction temperature approximately 25 °C lower than 2-ME-based precursors. Also a major benefit of water-based AlO_x precursor is that water is a nontoxic solvent and the application of water-based materials in solution-based electronics would certainly lead to a more environmentally friendly process. Considering the advantageous processing conditions of solution-processed AlO_x the obtained results clearly demonstrate that the aqueous combustion synthesis of dielectric materials and their

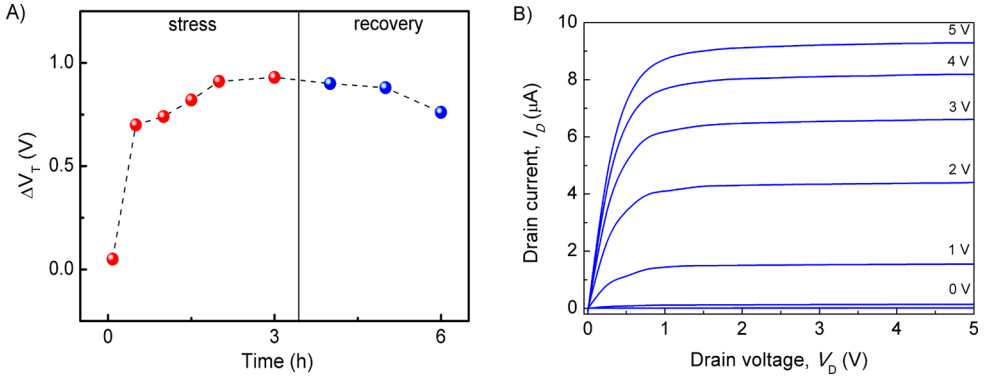

Figure 8. (A) Threshold voltage (V_T) variation of bottom gate water-based AlO_x TFTs with solution-based GZTO during a 2 MV cm^{-1} gate bias stress test, the dotted line is a guide for the eyes; (B) output characteristics obtained after 3 h recovery.

dx.doi.org/10.1021/am503872t | ACS Appl. Mater. Interfaces 2014, 6, 19592−19599

application in electronic devices is highly promising. In fact, 10 nm thick spin-coated AlO_x films were used together with solution-processed GZTO semiconductor to fabricate TFTs with very good performance, with the advantage of exhibiting considerably lower operating voltages because of high capacitance. Also a close to zero turn on voltage, 0.5 V, low subthreshold swing, 0.3 V dec^{-1}, and a saturation mobility of 1.3 $cm^2\ V^{-1}\ s^{-1}$ were obtained for water-based AlO_x TFTs. Moreover, thermal characterization indicates that by adjusting the reaction parameters, an ignition temperature bellow 200 °C can be attained for water based precursors which would be a remarkable advance in the development of low temperature insulator materials and is currently being investigated. Although leakage current of water-based AlO_x and I_{OFF} of the solution processed TFTs were still too high for what is required in AMTFT displays applications, successful preparation of aqueous AlO_x films by a relatively low-temperature solution process represents a significant achievement because it demonstrates the possibility for a low-cost, environmentally friendly production process. The versatility of solution combustion reaction and its applicability to other metal salts opens numerous possibilities for low-temperature solution synthesis of dielectric oxides that are crucial in the development of all solution-based flexible electronics.

■ ASSOCIATED CONTENT

Supporting Information

Figures S1 and S2 show FTIR spectra of water and 2-methoxyethanol solutions of initial reagents and AlO_x precursors. Figure S3 depicts AFM measurements of AlO_x thin films. Figure S4 represents the refractive index of AlO_x thin films. Figure S5 depicts capacitance-frequency characteristics of MIS devices with solution-based AlO_x thin films and Table S1 shows the frequency dependence of capacitance and relative permittivity of these films. Figure S6 shows the leakage current density of water-based p-Si/AlO_x/Al MIS. This material is available free of charge via the Internet at http://pubs.acs.org.

■ AUTHOR INFORMATION

Corresponding Authors

*E-mail: elvira.fortunato@fct.unl.pt.
*E-mail: ritasba@campus.fct.unl.pt.

Notes

The authors declare no competing financial interest.

■ ACKNOWLEDGMENTS

This work was funded by the Portuguese Science Foundation (FCT-MEC) through the projects EXCL/CTM-NAN/0201/2012 and PEst-C/CTM/LA0025/2013-14, and the European projects: ERC 2008 Advanced Grant (INVISIBLE contract 228144), ORAMA CP-IP 246334-2, POINTS NMP 263042 and i-FLEXIS ICT 611070. The authors acknowledge Pawel Wojcik, PhD for his imaging contribution to this paper.

■ REFERENCES

(1) Kim, M.-G.; Kanatzidis, M. G.; Facchetti, A.; Marks, T. J. Low-Temperature Fabrication of High-Performance Metal Oxide Thin-Film Electronics via Combustion Processing. *Nat. Mater.* **2011**, *10*, 382−388.

(2) Hennek, J. W.; Kim, M.-G.; Kanatzidis, M. G.; Facchetti, A.; Marks, T. J. Exploratory Combustion Synthesis: Amorphous Indium Yttrium Oxide for Thin-Film Transistors. *J. Am. Chem. Soc.* **2012**, *134*, 9593−9596.

(3) Hennek, J. W.; Smith, J.; Yan, A.; Kim, M.-G.; Zhao, W.; Dravid, V. P.; Facchetti, A.; Marks, T. J. Oxygen Getter" Effects on Microstructure and Carrier Transport in Low Temperature Combustion-Processed a-InXZnO (X = Ga, Sc, Y, La) Transistors. *J. Am. Chem. Soc.* **2013**, *135*, 10729−10741.

(4) Rim, Y. S.; Lim, H. S.; Kim, H. J. Low-Temperature Metal-Oxide Thin-Film Transistors Formed by Directly Photopatternable and Combustible Solution Synthesis. *ACS Appl. Mater. Interfaces* **2013**, *5*, 3565−3571.

(5) Han, S.-Y.; Herman, G. S.; Chang, C. Low-Temperature, High-Performance, Solution-Processed Indium Oxide Thin-Film Transistors. *J. Am. Chem. Soc.* **2011**, *133*, 5166−5169.

(6) Pasquarelli, R. M.; Ginley, D. S.; O'Hayre, R. Solution Processing of Transparent Conductors: From Flask to Film. *Chem. Soc. Rev.* **2011**, *40*, 5406−5441.

(7) Nayak, P. K.; Busani, T.; Elamurugu, E.; Barquinha, P.; Martins, R.; Hong, Y.; Fortunato, E. Zinc Concentration Dependence Study of Solution Processed Amorphous Indium Gallium Zinc Oxide Thin Film Transistors Using High-K Dielectric. *Appl. Phys. Lett.* **2010**, *97*, 183504−183504−3.

(8) Meyers, S. T.; Anderson, J. T.; Hung, C. M.; Thompson, J.; Wager, J. F.; Keszler, D. A. Aqueous Inorganic Inks for Low-Temperature Fabrication of ZnO TFTs. *J. Am. Chem. Soc.* **2008**, *130*, 17603−17609.

(9) Nayak, P. K.; Pinto, J. V.; Goncalves, G.; Martins, R.; Fortunato, E. Environmental, Optical, and Electrical Stability Study of Solution-Processed Zinc-Tin-Oxide Thin-Film Transistors. *J. Dispersion Technol.* **2011**, *7*, 640−643.

(10) Parthiban, S.; Elangovan, E.; Nayak, P. K.; Goncalves, A.; Nunes, D.; Pereira, L.; Barquinha, P.; Busani, T.; Fortunato, E.; Martins, R. Performances of Microcrystalline Zinc Tin Oxide Thin-Film Transistors Processed by Spray Pyrolysis. *J. Dispersion Technol.* **2013**, *9*, 825−831.

(11) Fortunato, E.; Barquinha, P.; Martins, R. Oxide Semiconductor Thin-Film Transistors: A Review of Recent Advances. *Adv. Mater.* **2012**, *24*, 2945−2986.

(12) Barquinha, P.; Pereira, L.; Martins, R.; Fortunato, E. *Transparent Electronics: From Materials to Devices*; John Wiley & Sons: New York, 2012.

(13) Pereira, L.; Barquinha, P.; Fortunato, E.; Martins, R.; Kang, D.; Kim, C. J.; Lim, H.; Song, I.; Park, Y. High K Dielectrics for Low Temperature Electronics. *Thin Solid Films* **2008**, *516*, 1544−1548.

(14) Pal, B. N.; Dhar, B. M.; See, K. C.; Katz, H. E. Solution-Deposited Sodium Beta-Alumina Gate Dielectrics for Low-Voltage and Transparent Field-Effect Transistors. *Nat. Mater.* **2009**, *8*, 898−903.

(15) Avci, N.; Smet, P.; Lauwaert, J.; Vrielinck, H.; Poelman, D. Optical and Structural Properties of Aluminium Oxide Thin Films Prepared by a Non-Aqueous Sol-Gel Technique. *J. Sol-Gel Sci. Technol.* **2011**, *59*, 327−333.

(16) Park, J. H.; Kim, K.; Yoo, Y. B.; Park, S. Y.; Lim, K.-H.; Lee, K. H.; Baik, H. K.; Kim, Y. S. Water Adsorption Effects of Nitrate Ion Coordinated Al2O3 Dielectric for High Performance Metal-Oxide Thin-Film Transistor. *J. Mater. Chem. C* **2013**, *1*, 7166−7174.

(17) Tardy, J.; Erouel, M.; Deman, A. L.; Gagnaire, A.; Teodorescu, V.; Blanchin, M. G.; Canut, B.; Barau, A.; Zaharescu, M. Organic Thin Film Transistors with HfO2 High-K Gate Dielectric Grown by Anodic Oxidation or Deposited by Sol-Gel. *Microelectron. Reliab.* **2007**, *47*, 372−377.

(18) Clima, S.; Pourtois, G.; Hardy, A.; Van Elshocht, S.; Van Bael, M. K.; De Gendt, S.; Wouters, D. J.; Heyns, M.; Kittl, J. A. Dielectric Response of Ta_2O_5, Nb_2O_5, and $NbTaO_5$ from First-Principles Investigations. *J. Electrochem. Soc.* **2010**, *157*, G20−G25.

(19) Hardy, A.; Van Elshocht, S.; Adelmann, C.; Conard, T.; Franquet, A.; Douhéret, O.; Haeldermans, I.; D'Haen, J.; De Gendt, S.; Caymax, M.; et al. Aqueous Solution-Gel Preparation of Ultrathin ZrO2 Films for Gate Dielectric Application. *Thin Solid Films* **2008**, *516*, 8343−8351.

(20) Jiang, K.; Anderson, J. T.; Hoshino, K.; Li, D.; Wager, J. F.; Keszler, D. A. Low-Energy Path to Dense HfO2 Thin Films with Aqueous Precursor. *Chem. Mater.* **2011**, *23*, 945−952.
(21) Jiang, K.; Meyers, S. T.; Anderson, M. D.; Johnson, D. C.; Keszler, D. A. Functional Ultrathin Films and Nanolaminates from Aqueous Solutions. *Chem. Mater.* **2013**, *25*, 210−214.
(22) Hwan Hwang, Y.; Seo, J.-S.; Moon Yun, J.; Park, H.; Yang, S.; Ko Park, S.-H.; Bae, B.-S. An "aqueous Route" for the Fabrication of Low-Temperature-Processable Oxide Flexible Transparent Thin-Film Transistors on Plastic Substrates. *NPG Asia Mater.* **2013**, *5*, e45.
(23) Gonzalez-Cortes, S. L.; Imbert, F. E. Fundamentals, Properties and Applications of Solid Catalysts Prepared by Solution Combustion Synthesis (SCS). *Appl. Catal. A Gen.* **2013**, *452*, 117−131.
(24) Shao, Z.; Zhou, W.; Zhu, Z. Advanced Synthesis of Materials for Intermediate-Temperature Solid Oxide Fuel Cells. *Prog. Mater. Sci.* **2012**, *57*, 804−874.
(25) Epifani, M.; Melissano, E.; Pace, G.; Schioppa, M. Precursors for the Combustion Synthesis of Metal Oxides from the Sol-Gel Processing of Metal Complexes. *J. Eur. Ceram. Soc.* **2007**, *27*, 115−123.
(26) Bae, E. J.; Kang, Y. H.; Han, M.; Lee, C.; Cho, S. Y. Soluble Oxide Gate Dielectrics Prepared Using the Self-Combustion Reaction for High-Performance Thin-Film Transistors. *J. Mater. Chem. C* **2014**, *2*, 5695.
(27) Pereira, L.; Águas, H.; Fortunato, E.; Martins, R. Nanostructure Characterization of High K Materials by Spectroscopic Ellipsometry. *Appl. Surf. Sci.* **2006**, *253*, 339−343.
(28) Schroder, D. K. *Semiconductor Material and Device Characterization*, 3rd ed.; John Wiley & Sons: New York, 2006.
(29) Jain, S. R.; Adiga, K. C.; Pai Verneker, V. R. A New Approach to Thermochemical Calculations of Condensed Fuel-Oxidizer Mixtures. *Combust. Flame* **1981**, *40*, 71−79.
(30) Sanchez-Rodriguez, D.; Farjas, J.; Roura, P.; Ricart, S.; Mestres, N.; Obradors, X.; Puig, T. Thermal Analysis for Low Temperature Synthesis of Oxide Thin Films from Chemical Solutions. *J. Phys. Chem. C* **2013**, *117*, 20133−20138.
(31) Kim, Y.-H.; Heo, J.-S.; Kim, T.-H.; Park, S.; Yoon, M.-H.; Kim, J.; Oh, M. S.; Yi, G.-R.; Noh, Y.-Y.; Park, S. K. Flexible Metal-Oxide Devices Made by Room-Temperature Photochemical Activation of Sol-Gel Films. *Nature* **2012**, *489*, 128−132.
(32) Nazrul Islam, M.; Monirul Islam, M.; Yeasmin, M. N. Viscosity of Aqueous Solutions of 2-Methoxyethanol, 2-Ethoxyethanol, and Ethanolamine. *J. Chem. Thermodyn.* **2004**, *36*, 889−893.
(33) Davis, S.; Gutiérrez, G. Structural, Elastic, Vibrational and Electronic Properties of Amorphous Al2O3 from Ab Initio Calculations. *J. Phys.: Condens. Matter* **2011**, *23*, 495401.
(34) Goebbert, D. J.; Garand, E.; Wende, T.; Bergmann, R.; Meijer, G.; Asmis, K. R.; Neumark, D. M. Infrared Spectroscopy of the Microhydrated Nitrate Ions NO3 (H2O)1−6. *J. Phys. Chem. A* **2009**, *113*, 7584−7592.
(35) Robertson, J. High Dielectric Constant Oxides. *Eur. Phys. J. Appl. Phys.* **2004**, *28*, 265−291.
(36) Avis, C.; Jang, J. High-Performance Solution Processed Oxide TFT with Aluminum Oxide Gate Dielectric Fabricated by a Sol-Gel Method. *J. Mater. Chem.* **2011**, *21*, 10649−10652.
(37) Barquinha, P.; Pereira, L.; Gonçalves, G.; Martins, R.; Fortunato, E.; Kuscer, D.; Kosec, M.; Vilà, A.; Olziersky, A.; Morante, J. R. Low-Temperature Sputtered Mixtures of High K and High Bandgap Dielectrics for GIZO TFTs. *J. Soc. Inf. Dispersion* **2010**, *18*, 762−772.